

**RETO GIERÉ**

Titanian Clinohumite and Geikielite in Marbles  
from the Bergell Contact Aureole

## Titanian clinohumite and geikielite in marbles from the Bergell contact aureole

Reto Gieré

Institut für Mineralogie und Petrographie, ETH-Zentrum, CH-8092 Zürich, Switzerland

**Abstract.** The assemblage titanian clinohumite + forsterite + spinel + calcite is widespread in marbles from the eastern Bergell contact aureole (Switzerland/Italy). The Bergell titanian clinohumites vary considerably in composition ( $\text{TiO}_2$ : 0.19 to 2.05 wt%, F: 2.2 to 3.4 wt%). Electron microprobe analyses show that the titanian clinohumites contain less than detectable amounts of Co, Cu, Ni, Zn, Al, Cr and Cl. No trace of ferric iron could be detected by Moessbauer spectroscopy. Moreover, the Moessbauer spectra indicate that  $\text{Fe}^{2+}$  occurs only in one of the five octahedral positions in the crystal structure of the studied titanian clinohumite. Under the conditions of the contact metamorphism (600–650°C, 3 kb total pressure) the compositional variation along the exchange vector  $\text{TiO}_2\text{M}_{-1}(\text{OH},\text{F})_2$  takes place at constant  $x_{\text{OH}}$  which is fixed by the pore fluid. Titanian clinohumite sometimes contains geikielite inclusions which strongly fractionate Fe and Mn relative to titanian clinohumite. The geikielites from the Bergell marbles are poor in  $\text{Cr}_2\text{O}_3$ ,  $\text{Fe}_2\text{O}_3$  and MnO, and thus different from those found in carbonatites, kimberlites and serpentinized ultramafic rocks.

### Introduction

Titanian varieties of the humite group minerals are quite common in metamorphic carbonate rocks and have been found at numerous localities (Rankama 1938; Sahama 1953; Muthuswami 1958; Bradshaw and Leake 1964; Moore and Kerrick 1976; Rice 1980; Bucher-Nurminen 1982; Ehlers and Hoinkes 1987). In marbles from the eastern Bergell contact aureole (Switzerland/Italy) humite minerals were first mentioned by Cornelius (1915). Later, Déverin (1937), Wenk (1963), Trommsdorff (1966), Bucher-Nurminen (1976, 1977) and Gieré (1984) described parageneses with forsterite, spinel, tremolite, chlorite, phlogopite, dolomite and calcite.

Geikielite, the rare magnesium analog of ilmenite, occurs as an accessory mineral in rocks with high Mg/Fe ratios. It is found in serpentinized ultramafic rocks (Kashin 1937; Efremov 1954; Trommsdorff and Evans 1980; Dietrich et al. 1986), in kimberlites (Mitchell 1973, 1977; Haggerty 1975) in carbonatites (Mitchell 1978), in metasomatically altered iron ores associated with carbonatites (Zhuravleva et al. 1976) and in metamorphosed impure magnesian limestones (Murdoch and Fahey 1949; Wise 1959; Cressey

1986; Ehlers and Hoinkes 1987). Geikielite has also been reported from the gem gravels of Sri Lanka (Crook and Jones 1906).

The Tertiary Bergell calc-alkaline intrusives contain along their eastern margin large inclusions of banded marbles with a wide variety of contact metamorphic mineral assemblages (Gieré 1985, see compilation p. 73). In this paper the assemblage titanian clinohumite + forsterite + spinel + calcite (Fig. 1) will be described. Electron microprobe analyses of titanian clinohumite and geikielite, as well as Moessbauer spectra of  $^{57}\text{Fe}$  in titanian clinohumite are presented.

### Petrography

Titanian clinohumite (Ti-Cl) occurs predominantly as megacrysts up to 2 cm in diameter. Due to compositional variation the intensity of the colourless to yellow pleochroism varies patchily within individual crystals. No regular zoning patterns are recognizable. No titanian chondrodite was observed in the studied samples. Irregular intergrowths of Ti-Cl with near-endmember forsterite are very common. Both forsterite and Ti-Cl contain parallel bands of tiny fluid and opaque solid inclusions that cross the grain boundaries (Fig. 1). Poikiloblastic megacrysts of Ti-Cl and forsterite enclose calcite and pale green, idiomorphic spinel rich in  $\text{MgAl}_2\text{O}_4$ . Calcite with straight to curved grain boundaries forms the matrix of these marbles. Dolomite is only rarely present in the studied mineral assemblage. The matrix shows a granoblastic polygonal texture.

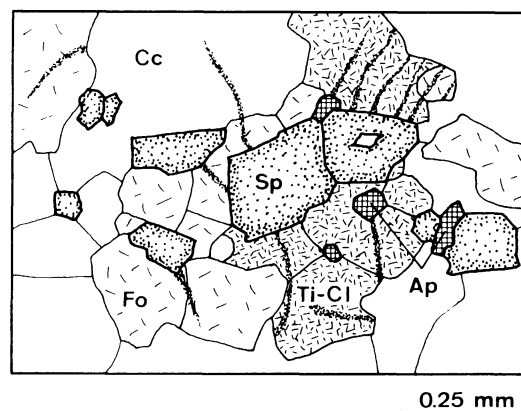


**Fig. 1.** Drawing from thin section showing the paragenesis titanian clinohumite (Ti-Cl) + forsterite (Fo) + spinel (Sp) + calcite (Cc) and accessory fluorapatite (Ap)

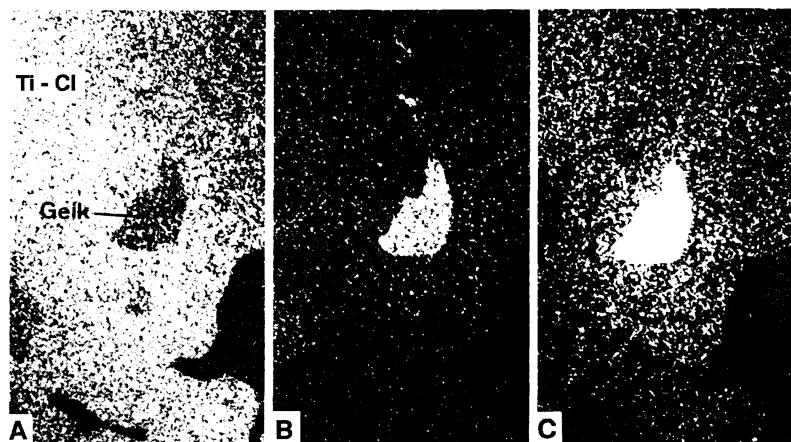


**Fig. 2.** X-ray scanning pictures of titanian clinohumite (*Ti-Cl*) with an inclusion of geikielite (*Geik*). Largest diameter of geikielite is 0.1 mm. **A** Mg-K $\alpha$ , **B** Fe-K $\alpha$ , **C** Ti-K $\alpha$

**Table 1.** Electron microprobe analyses of Bergell titanian clinohumites (five single spot analyses in different crystals of sample ROS 8)

wt%	1	2	3	4	5	Average relative error ( $1\sigma$ ) in %
SiO <sub>2</sub>	37.8	37.9	37.7	37.6	37.6	0.5
TiO <sub>2</sub>	1.60	0.20	0.65	1.10	1.99	2.0 (at 0.2% level) 0.6 (at 2% level)
FeO <sup>a</sup>	2.49	2.43	2.53	2.56	2.50	1.2
MnO	0.20	0.19	0.19	0.18	0.19	3.9
MgO	54.8	55.7	55.5	55.0	54.3	0.2
CaO	0.02	0.02	0.02	0.02	0.02	6.8
F	2.5	3.1	2.9	2.7	2.2	4.3 (at 2.3% level) 3.7 (at 3% level)
OH <sub>corr</sub>	2.4	2.5	2.5	2.5	2.5	
F $\equiv$ O	-1.1	-1.3	-1.2	-1.1	-0.9	
Total <sup>b</sup>	100.7	100.7	100.8	100.6	100.4	
Number of ions on the basis of 13 cations						
Si	3.993	3.991	3.976	3.977	3.995	
Ti	0.127	0.016	0.051	0.088	0.159	
Fe <sup>2+</sup>	0.220	0.214	0.224	0.227	0.222	
Mn	0.018	0.017	0.017	0.016	0.018	
Mg	8.639	8.760	8.730	8.691	8.604	
Ca	0.002	0.002	0.002	0.002	0.002	
F	0.835	1.033	0.962	0.909	0.746	
OH <sub>calc</sub>	0.912	0.938	0.941	0.921	0.937	
x <sub>Fe</sub>	0.025	0.024	0.025	0.025	0.025	
x <sub>Ti</sub>	0.127	0.016	0.051	0.088	0.159	
x <sub>F</sub>	0.418	0.516	0.481	0.454	0.373	
x <sub>OH</sub>	0.456	0.469	0.471	0.461	0.468	
Charge						
$\sum +$	34.238	34.014	34.054	34.132	34.308	
$\sum -$	34.255	34.035	34.107	34.182	34.319	
Stoichiometry						
S1	0.998	0.997	0.991	0.992	0.998	
S2	1.996	1.993	1.983	1.983	1.997	

<sup>a</sup> Total Fe as FeO

<sup>b</sup> Cl < 0.01wt%, Co < 0.01wt%, CuO < 0.02wt%, NiO < 0.02wt%, ZnO < 0.03wt%, Al<sub>2</sub>O<sub>3</sub> < 0.01wt%, Cr<sub>2</sub>O<sub>3</sub> < 0.01wt%

OH<sub>corr</sub> = OH<sub>calc</sub> converted to corresponding wt% OH<sup>-</sup>

OH<sub>calc</sub> = 2/9(Mg + Fe + Mn + Ca + Ni + Zn + Ti) - 2Ti - F (Jones et al. 1969)

S1 = 2Si : (8/9M<sub>Ti</sub>) = 2Si : (octahedral cations in the M<sub>2</sub>SiO<sub>4</sub>-portion of the structure). M<sub>Ti</sub> = Ti +  $\sum M^{2+}$

S2 = Si : (OH + F + O<sub>Ti</sub>), where O<sub>Ti</sub> = 2Ti since Ti is ordered into the M<sub>3</sub>-site (Ribbe 1979)

**Table 2.** Electron microprobe analyses of Bergell geikielites (single spot analyses in three different crystals of sample ROS 8, Nos. 3 and 4 from same crystal)

wt%	1	2	3	4	Average relative error (1 $\sigma$ ) in %
TiO <sub>2</sub>	58.0	58.3	58.5	58.2	0.1
Cr <sub>2</sub> O <sub>3</sub>	0.03	0.05	0.04	0.05	14.6
Fe <sub>2</sub> O <sub>3</sub> <sup>a</sup>	3.0	2.4	2.0	2.2	
FeO	18.3	18.7	18.9	18.9	0.4
MnO	1.65	1.56	1.52	1.57	1.5
MgO	18.0	18.2	18.3	18.1	0.3
CaO	0.07	0.01	0.01	0.01	7.9
SiO <sub>2</sub>	<0.24	0.26	0.4	0.4	16.8
Total	99.1	99.5	99.7	99.4	
Number of cations assuming stoichiometry and charge balance					
Ti	0.975	0.974	0.975	0.971	
Cr	0.001	0.001	0.001	0.001	
Fe <sup>3+</sup>	0.050	0.040	0.033	0.037	
Fe <sup>2+</sup>	0.341	0.348	0.351	0.351	
Mn	0.031	0.029	0.029	0.030	
Mg	0.600	0.602	0.604	0.600	
Ca	0.002	0.000	0.000	0.000	
Si	0.000	0.006	0.008	0.010	
Endmember proportions (mole%)					
Hematite	2.5	1.9	1.6	1.8	
Ilmenite	34.2	34.8	35.1	35.1	
Geikielite	60.2	60.3	60.4	60.1	
Pyrophanite	3.1	2.9	2.9	3.0	

<sup>a</sup> Calculated

Fluor-apatite and geikielite occur as accessory phases. The small apatite crystals with 2.2–3.1 wt% F are usually idiomorphic and closely associated with Ti-Cl (Fig. 1). Geikielite has been found as small (0.1–0.4 mm) inclusions in Ti-Cl (Fig. 2). Occasionally, euhedral geikielite grains may reach 3 mm in diameter (Bedogné, personal communication).

### Analytical procedure

Analyses were performed using an automated ARL SEMQ microprobe, operated at an acceleration potential of 15 kV and a sample current of 20 nA (measured on brass), yielding a beam size of 0.2  $\mu$ m. For quantitative analyses six crystal X-ray spectrometers and an X-ray energy dispersive analyzer (TN 2000 by Tracor Northern) were applied simultaneously. The X-ray data collection time was 40 s. Samples and standards were coated with 200 Å of carbon. The reference standard for Si and Mg was a natural forsterite which was carefully checked against other standards for its composition. For the other elements natural and synthetic silicates (Mn, Ca, Ti, Ni, Cl, F), oxides (Fe, Zn, Cu, Al, Cr) and sulfides (Co) were used as standards. The relative errors due to counting statistics are listed in Tables 1 and 2. The raw data were corrected on-line for drift, dead-time and background. Full corrections for X-ray absorption, X-ray fluorescence by characteristic and continuous excitation, atomic number effect, backscatter losses and ionisation-penetration losses were applied to the data by a ZAF computer program at the ETH Zürich.

### Compositional variation in titanian clinohumite

The humite group minerals can be described with the following general formula:



where  $M = \text{Mg, Fe, Mn, Ca, Zn, Ni}$ , and  $n = 1$  for norbergite,  $n = 2$  for chondrodite,  $n = 3$  for humite and  $n = 4$  for clinohumite (Jones et al. 1969). The chemical composition of Ti-Cl (13 cations) is characterized by atomic fractions defined as:  $x_{\text{Fe}} = \text{Fe} / \sum M^{2+}$ ,  $x_{\text{Ti}} = \text{Ti}$  per formula unit of 13 cations ( $x_{\text{Ti}} < 0.5$ , Ribbe 1979) and  $x_{\text{F}} = 0.5\text{F}$  per formula unit. The exchange vectors  $\text{FeMg}_{-1}$ ,  $\text{OH}_{-1}$  and  $\text{TiO}_2 M_{-1} (\text{OH},\text{F})_{-2}$  (Ribbe et al. 1968; Jones et al. 1969) express the three main substitutions causing compositional variation in Ti-Cl.

A calcite marble rich in Ti-Cl and spinel, but containing only small amounts of forsterite, was selected to examine the compositional variation in Ti-Cl. The sample (sample ROS 8) was collected from a marble inclusion in the Bergell tonalite in the upper Valle Sissone, Italy (Swiss coordinates: 776.400/130.500).

The Ti-Cl cell dimensions were determined with an X-ray diffraction camera of the Guinier-Hägg type using Cr-K $\alpha$  radiation. From the reflexions (102), (112), (004), (113) and (1 $\bar{3}$ ) the following values were obtained by using a computer program based on the mean least squares fit method:  $a_0 = 4.74 \text{ \AA}$ ,  $b_0 = 10.23 \text{ \AA}$ ,  $c_0 = 13.66 \text{ \AA}$ , and  $\beta = 100.91^\circ$ . They correspond well to the values given for Ti-Cl by Jones et al. (1969) and Robinson et al. (1973).

From the electron microprobe analyses (five are shown in Table 1) it is evident that the Bergell Ti-Cl show only insignificant (less than 2%, 60 analyses) deviations from ideal stoichiometry (cf., stoichiometry ratios S1 and S2, Table 1). Thus, fine scale intergrowths of different humite minerals, as observed by Müller and Wenk (1978) and White and Hyde (1982), are not indicated by the microprobe data. The Bergell Ti-Cl show a considerable variation in their TiO<sub>2</sub>- and F-contents (TiO<sub>2</sub>: 0.19 to 2.05 wt%, F: 2.2 to 3.4 wt%), but only minor variation along the exchange vector  $\text{FeMg}_{-1}$ . They have a constant average  $x_{\text{OH}}^1$  of  $0.46 \pm 0.02$  (60 analyses), corresponding to 2.5 wt% OH<sup>-</sup>. Titanium is usually distributed inhomogeneously within individual crystals but no symmetric zoning pattern can be observed. Inhomogeneous titanium distribution was also found by Bucher-Nurminen (1977) and by Ehlers and Hoinkes (1987), and seems to be characteristic for Ti-Cl occurring in marbles.

The Bergell Ti-Cl contain only small amounts of MnO and CaO, and the concentrations of Co, Cu, Ni, Zn, Al and Cr are below microprobe detection limit (see Table 1). Although nearly all of the published bulk chemical analyses of humite minerals report ferric iron, the Ti-Cl from the studied sample are free of Fe<sup>3+</sup>. This is demonstrated by Moessbauer spectra of <sup>57</sup>Fe taken at 78K and at 295K. Both spectra exhibit one single doublet assigned to ferrous iron (Fig. 3). The sharp resonant absorption lines of the Fe<sup>2+</sup> doublet (0.31 mm/s and 0.32 mm/s at 78K, and 0.29 mm/s and 0.36 mm/s at 295K for the low and high velocity peaks, respectively; the values are full widths at half peak height) indicate that Fe<sup>2+</sup> apparently occurs only in one of the five octahedral positions in the crystal structure of Ti-Cl from this sample. More spectra of different samples should be studied for more precise crystallographic information. In contrast to Ti-Cl, the coexisting geikielites always contain small amounts of Fe<sup>3+</sup> (Table 2). Similar

<sup>1</sup>  $x_{\text{OH}} = 0.5 \text{ OH}_{\text{calc}}$ , where  $\text{OH}_{\text{calc}} = 2/9(\text{Mg} + \text{Fe} + \text{Mn} + \text{Ca} + \text{Ni} + \text{Zn} + \text{Ti}) - 2\text{Ti} - \text{F}$  (Jones et al. 1969)

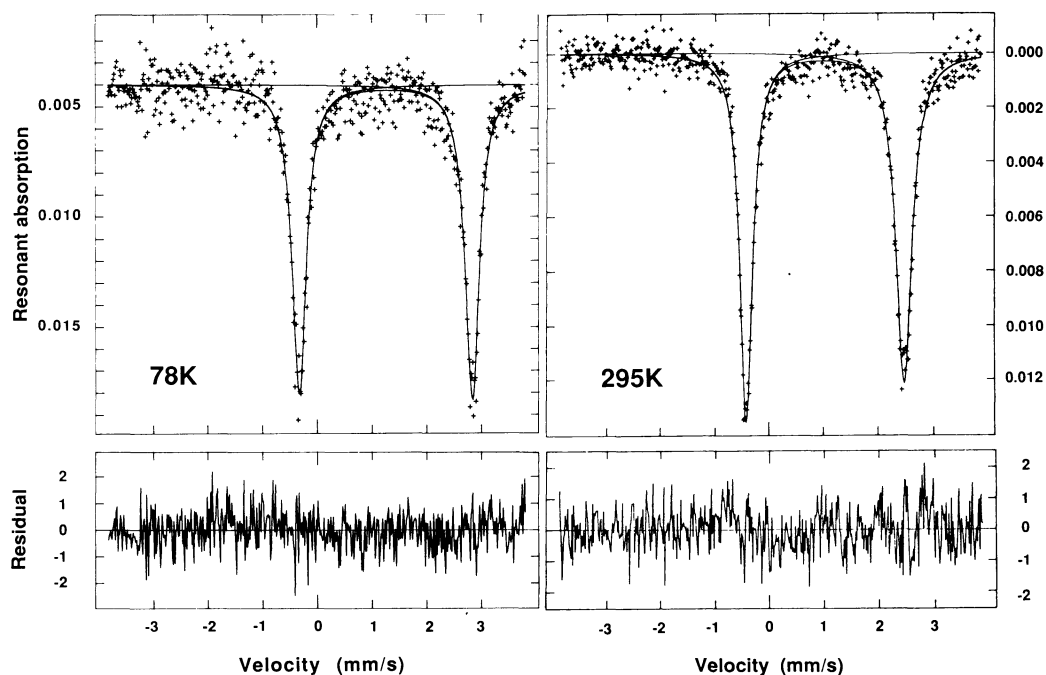


**Fig. 3.** Mössbauer spectra of  $^{57}\text{Fe}$  in a powdered sample of the Bergell titanian clinohumite (sample ROS 8) showing one doublet of  $\text{Fe}^{2+}$  at 78K and at 295K. The sharp resonance absorption lines of the  $\text{Fe}^{2+}$  doublet indicate one crystallographic position for  $\text{Fe}^{2+}$  in the structure. No trace of  $\text{Fe}^{3+}$  can be observed (cf., residual, i.e., the difference between the computed intensity of the fitted Lorentzian curve and the data). The isomer shift of the doublet is 1.26 mm/s and 1.14 mm/s, the nuclear quadrupole splitting 3.16 mm/s and 2.90 mm/s at 78K and 295K, respectively

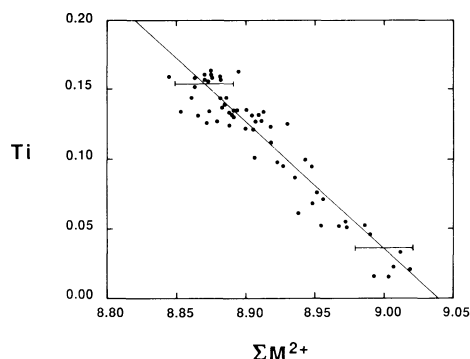


**Fig. 4.** Ti versus  $\sum M^{2+}$  in the Bergell titanian clinohumites. The diagram shows the one-for-one cation basis of  $\text{TiO}_2M_{-1}F_{-2}$ . Slope of regression line is  $-0.92$  (correlation coefficient:  $-0.95$ ). Error bars represent the relative error due to counting statistics ( $1\sigma$ ). Error bar for Ti is smaller than symbols

amounts of  $\text{Fe}^{3+}$  are also present in spinel ( $0.7\text{--}4.0$  wt%  $\text{Fe}_2\text{O}_3$ )<sup>2</sup>.

Within the limits of analytical error (see Table 1) Ti and  $\sum M^{2+}$  correlate negatively along a line of slope  $-1$ , i.e.,  $\text{Ti} + \sum M^{2+} = \text{constant}$  (Fig. 4). This confirms the one-for-one cation substitution expressed by the exchange vector  $\text{TiO}_2M_{-1}(\text{OH},\text{F})_{-2}$  (cf., Evans and Trommsdorff 1983, Fig. 2). During this exchange, MnO and CaO remain almost constant ( $\text{MnO} = 0.20 \pm 0.02$  wt%,  $\text{CaO} = 0.02 \pm 0.01$  wt%). Since the slope of the regression line for Ti versus Mg is significantly lower (slope:  $-0.79 \pm 0.09$ , correla-

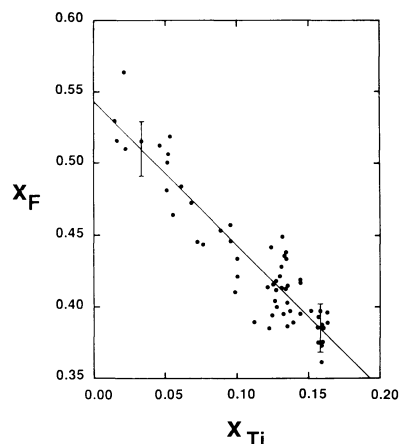


**Fig. 5.**  $x_{\text{F}}$  versus  $x_{\text{Ti}}$  in the Bergell titanian clinohumites. The regression line (slope:  $-1.01$ , correlation coefficient:  $-0.93$ ) corresponds to  $x_{\text{OH}} = 0.46$ . Error bars represent the relative error due to counting statistics ( $1\sigma$ ). Error bar for Ti is smaller than symbols

tion coefficient:  $-0.92$ ) than for Ti versus  $\sum M^{2+}$ , a positive correlation should be found between Ti and Fe. In the studied sample however, this correlation is only weak (see below).

Figure 5 shows that  $x_{\text{F}}$  and  $x_{\text{Ti}}$  correlate negatively along a line of slope  $-1$  implying a constant  $x_{\text{OH}}$  of 0.46 during the exchange along  $\text{TiO}_2M_{-1}(\text{OH},\text{F})_{-2}$ . The value of  $x_{\text{OH}}$ , given by the  $x_{\text{F}}$ -intercept of the regression line, is identical with the average  $x_{\text{OH}}$ , which was calculated directly from the microprobe analyses by using the equation of Jones et al. (1969; see above). These observations indicate that the coupled substitution  $\text{Ti} + 2\text{O} = \text{M} + 2(\text{OH},\text{F})$  can essentially be written as  $\text{Ti} + 2\text{O} = \text{M} + 2\text{F}$ , i.e., that the operative exchange vector is  $\text{TiO}_2M_{-1}F_{-2}$ . Chlorine has not

<sup>2</sup> Average spinel composition:  $(\text{Mg}_{0.93}\text{Fe}_{0.07}^{2+}) (\text{Al}_{1.93}\text{Fe}_{0.07}^{3+})\text{O}_4$ ;  $\text{TiO}_2 < 0.02$  wt%,  $\text{MnO} < 0.03$  wt%

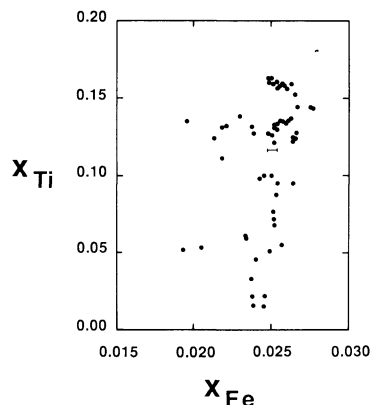


Fig. 6.  $x_{\text{Ti}}$  versus  $x_{\text{Fe}}$  in the Bergell titanian clinohumites (all stoichiometric). Error bars represent the relative error due to counting statistics ( $1\sigma$ ). Error bar for Ti is smaller than symbols

to be considered, since its concentration is below microprobe detection limit in all analyzed Ti-Cl (Cl < 0.01 wt%). Coexisting apatite however, always contains small amounts of Cl (0.2–0.3 wt% Cl).

The exchange along  $\text{TiO}_2\text{M}_{-1}\text{F}_{-2}$  takes place at significantly lower  $x_{\text{OH}}$  than in Ti-Cl occurring in metaperidotites from Cima di Gagnone, Switzerland (Evans and Trommsdorff 1983) and in marbles from the Oetztal basement, Austria (Ehlers and Hoinkes 1987). These data suggest an external control of  $x_{\text{OH}}$ . The only other hydrous phase present in the studied paragenesis is fluor-apatite (2.2–3.1 wt% F). Fluorite was not observed. Thus the exchange chemical potential of  $\text{OHF}_{-1}$  in Ti-Cl could be determined either by fluor-apatite or by the pore fluid. Since apatite is not always present, it is suggested here that  $x_{\text{OH}}$  is controlled by the pore fluid.

In Fig. 6  $x_{\text{Ti}}$  and  $x_{\text{Fe}}$  do not follow a specific trend. An analogous scatter is also found in the diagram  $x_{\text{F}}$  versus  $x_{\text{Fe}}$ . The  $1\sigma$ -error bar in Fig. 6 shows that the scatter is not due to the analytical error. Nor can it be explained by non-stoichiometry, since all data points represent stoichiometric Ti-Cl. These observations indicate that the exchange vectors  $\text{MgFe}_{-1}$  and  $\text{TiO}_2\text{M}_{-1}\text{F}_{-2}$  are nearly uncorrelated.

Evans and Trommsdorff (1983), studying the compositional variation of Ti-Cl in metaperidotites, suggested that olivine serves as a buffer for the Mg/Fe ratio in Ti-Cl. In contrast to those metaperidotites, the studied Bergell marble contains only very minor amounts of ferromagnesian phases other than Ti-Cl, viz. olivine and dolomite. Thus the exchange chemical potential of  $\text{FeMg}_{-1}$  could be equilibrated only locally. The scatter in Fig. 6 then might be caused by Ti-Cl which does not coexist with olivine or dolomite.

Ti-Cl with geikielite inclusions is highest in  $\text{TiO}_2$  (Table 1, analysis 5). In the vicinity of these inclusions the Ti-Cl show only minor compositional variation and have a nearly constant  $x_{\text{Ti}}$  ( $x_{\text{Ti}} = 0.159 \pm 0.002$ ). At this  $x_{\text{Ti}}$  the  $K_D^3$ -values for Mg-Fe and Mg-Mn partition between coexistent Ti-Cl and geikielite show that both Fe and Mn are strongly partitioned into geikielite (range of  $K_D^{\text{Mg-Fe}} = 22.3\text{--}23.0$ , range of  $K_D^{\text{Mg-Mn}} = 24.5\text{--}25.8$ ). The effect of  $x_{\text{Ti}}$  on the  $K_D$ -values can-

$${}^3 K_D^{\text{Mg-Fe}} = \frac{([\text{Mg}] / [\text{Fe}])^{\text{Ti-Cl}}}{([\text{Mg}] / [\text{Fe}])^{\text{Geik}}} \quad {}^3 K_D^{\text{Mg-Mn}} = \frac{([\text{Mg}] / [\text{Mn}])^{\text{Ti-Cl}}}{([\text{Mg}] / [\text{Mn}])^{\text{Geik}}}$$

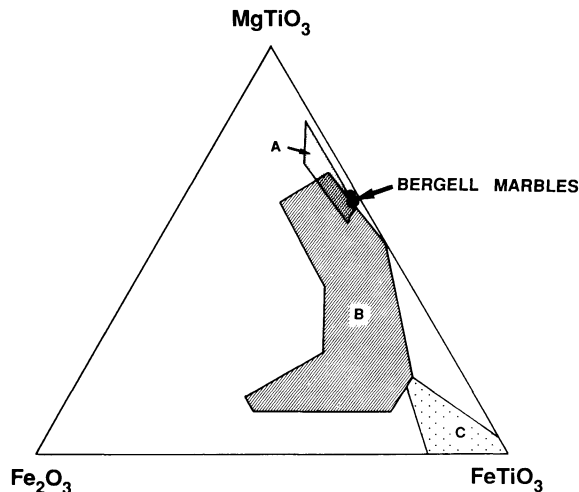


Fig. 7. Composition of the Bergell geikielites in the triangular plot  $\text{Fe}_2\text{O}_3\text{-FeTiO}_3\text{-MgTiO}_3$  (mole%). For comparison other data are given: *Field A* ilmenites from Jacupiranga carbonatite (Mitchell 1978), *Field B* ilmenites from kimberlites (Mitchell 1973, 1977; Haggerty 1975), *Field C* ilmenites from lamprophyres, granites, basalts and carbonatites (Prins 1972; Haggerty 1976; Bergstøl 1972; Czamanske and Mihalik 1972; Gieré 1984)

not be specified, because  $x_{\text{Ti}}$  is nearly constant around the geikielite inclusions.

### Composition of geikielite

All analyzed ilmenites contain more than 50 mole%  $\text{MgTiO}_3$  and thus fall within the compositional range of geikielite. Four representative electron microprobe analyses are shown in Table 2. From these analyses it can be seen that the Bergell geikielites exhibit a very restricted compositional range. They are poor in  $\text{Cr}_2\text{O}_3$  and  $\text{Fe}_2\text{O}_3$ , and contain rather small amounts of MnO.

In Fig. 7 the compositional field of the Bergell geikielites overlaps those of ilmenites from kimberlites (Mitchell 1973, 1977; Haggerty 1975) and from the Jacupiranga carbonatites (Mitchell 1978). From the kimberlite ilmenites however, they can be distinguished on the basis of their extremely low  $\text{Cr}_2\text{O}_3$ -content (see Table 2). Kimberlite ilmenites typically contain 0.1–2.5 wt%  $\text{Cr}_2\text{O}_3$ . High  $\text{Cr}_2\text{O}_3$ -concentrations have also been reported by Kashin (1937) and Efremov (1954) from geikielites associated with chrome-spinel deposits in serpentinites.

On the other hand, the Bergell geikielites can be distinguished from both the Jacupiranga geikielites and the kimberlite ilmenites on the basis of their pyrophanite-component (Fig. 8). Figure 8 also shows that the Bergell geikielites differ in composition from those occurring in other marbles and rock types.

### Discussion

In the marbles from the eastern Bergell contact aureole Ti-Cl always contains fluorine. By contrast, fluorine-free Ti-Cl with much higher  $\text{TiO}_2$ -contents ( $\text{TiO}_2$ : 4.24 to 5.59 wt%), occurring in the adjacent Malenco serpentinites, has been shown to break down within the same contact aureole to olivine+magnesian ilmenite (or geikielite)+ magnetite (Trommsdorff and Evans 1980). Outside this

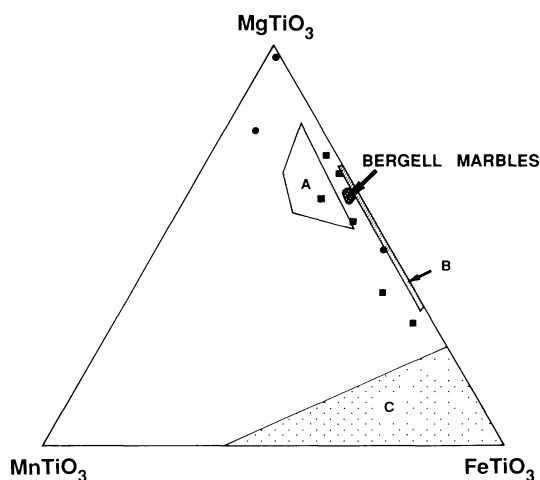


**Fig. 8.** Composition of the Bergell geikielites in the triangular plot  $\text{MnTiO}_3$ - $\text{FeTiO}_3$ - $\text{MgTiO}_3$  (mole%). Explanation of *Fields A, B* and *C* see Fig. 7. Geikielites from serpentinized ultrabasic rocks (*squares* Kashin 1937, Efremov 1954, Trommsdorff and Evans 1980, Dietrich et al. 1986) and other marbles (*dots* Murdoch and Fahey 1949, Cressey 1986, Ehlers and Hoinkes 1987) are plotted for comparison

aureole F-free Ti-Cl seems to be a stable member of the regional metamorphic parageneses in those serpentinites (DeQuervain 1938). Fluorine-bearing Ti-Cl occurs also in ultramafic rocks that underwent garnet-lherzolite metamorphism in the Central Alps (800°C, 25kb, Evans and Trommsdorff 1983). These observations confirm that the presence of fluorine has a strong effect in increasing the stability of titanian OH-clinohumite (Rice 1980).

Engi and Lindsley (1980) investigated experimentally the upper thermal stability limit of a natural, F-free Ti-Cl from the Malenco serpentinites, and modelled quantitatively the effects of the  $\text{OH}_{-1}$  substitution. Their calculated reaction curves indicate that under the metamorphic conditions in the Bergell marbles (600–650°C, 3kb total pressure, cf., Bucher-Nurminen 1977, Trommsdorff and Evans 1980) Ti-Cl is relatively more stable than olivine + geikielite + vapor *only* if  $x_{\text{F}} > 0.1$ . This requirement is fulfilled by all analyzed Ti-Cl. Although  $x_{\text{Ti}}$  in the Bergell Ti-Cl is always smaller than the  $x_{\text{Ti}}$  used by Engi and Lindsley (1980) for their calculations, no textural evidence for a breakdown of Ti-Cl was found.

**Acknowledgements.** The author would like to thank Prof. P.H. Ribbe (Virginia Polytechnic Institute), Prof. B.W. Evans (University of Washington), Prof. R.H. Mitchell (Lakehead University), Prof. S. Hafner (Philipps-Universität Marburg), Prof. V. Trommsdorff (ETH Zürich) and Prof. M. Engi (Universität Bern) for their careful and critical reviews of the manuscript. I am particularly indebted to Prof. S. Hafner for undertaking Moessbauer spectroscopy on my sample and for calculating the cell parameters of Ti-Cl. The financial support of the Schweizerischer Nationalfonds (No. 2.601-0.85) is gratefully acknowledged.

## References

- Bergstøl S (1972) The jacupirangite at Kodal, Vestfold, Norway. A potential magnetite, ilmenite and apatite ore. *Miner Deposita* 7:233–246
- Bradshaw R, Leake BE (1964) A chondrodite-humite-spinel marble from Sørfinnset, near Glomfjord, northern Norway. *Mineral Mag* 33:1066–1080
- Bucher-Nurminen K (1976) Chlorit-Spinell Paragenesen aus Dolomitmarmoren des Bergell-Ostrand. *Schweiz Mineral Petrogr Mitt* 56:95–100
- Bucher-Nurminen K (1977) Hochmetamorphe Dolomitmarmore und zonierte metasomatische Adern im oberen Val Sissone (Provinz Sondrio, Norditalien). Ph.D. thesis, No. 5910, ETH Zürich
- Bucher-Nurminen K (1982) On the mechanism of contact aureole formation in dolomitic country rock by the Adamello intrusion (northern Italy). *Am Mineral* 67:1101–1117
- Cornelius HP (1915) Geologische Beobachtungen in den italienischen Teilen des Albigna-Disgraziamaassivs. *Geol Rundsch* 6:166–177
- Cressey G (1986) Geikielite and perovskite in serpentine-brucite marble from Baltistan, Northern Areas (Kashmir), Pakistan. *Mineral Mag* 50:345–346
- Crook T, Jones BM (1906) Geikielite and the ferro-magnesian titanates. *Mineral Mag* 14:160–166
- Czamaske GK, Mihalik P (1972) Oxidation during magmatic differentiation. Finnmarka complex, Oslo area, Norway. Part I. The opaque oxides. *J Petrol* 13:493–509
- De Quervain F (1938) Zur Kenntnis des Titanklinohumites (Titanolivin). *Schweiz Mineral Petrogr Mitt* 18:591–605
- Déverin L (1937) Composition minéralogique d'un calcaire à silicates de la bordure du massif de Bergell. Gisements de humites sur territoire Suisse. *Schweiz Mineral Petrogr Mitt* 17:531
- Dietrich H, Koller F, Richter W, Kiesel W (1986) Petrologie und Geochemie des Rodingitvorkommens vom Isflitzfall (Dorfertal, Hohe Tauern). *Schweiz Mineral Petrogr Mitt* 66:163–192
- Efremov N (1954) Geikielite from Mount Jemorakly-Tube, North Caucasus, USSR. *Am Mineral* 39:395–396
- Ehlers K, Hoinkes G (1987) Titanian chondrodite and clinohumite in marbles from the Oetzal crystalline basement. *Mineral Petrol* 36:13–25
- Engi M, Lindsley DH (1980) Stability of titanian clinohumite: experiments and thermodynamic analysis. *Contrib Mineral Petrol* 72:415–424
- Evans BW, Trommsdorff V (1983) Fluorine hydroxyl titanian clinohumite in Alpine recrystallized garnet peridotite: compositional controls and petrologic significance. *Am J Sci* 283A:355–369
- Gieré R (1984) Geologie und Petrographie des Bergell Ostrand. Diploma thesis, ETH Zürich
- Gieré R (1985) Metasedimente der Suretta-Decke am Ost- und Südostrand der Bergeller Intrusion: Lithostratigraphische Korrelation und Metamorphose. *Schweiz Mineral Petrogr Mitt* 65:57–78
- Haggerty SE (1975) The chemistry and genesis of opaque minerals in kimberlite. *Phys Chem Earth* 9:295–307
- Haggerty SE (1976) Opaque mineral oxides in terrestrial igneous rocks. In: Rumble DH (ed) *Oxide minerals*. Mineral Soc Am Short Course Notes 3:Hg 101–Hg 300
- Jones NW, Ribbe PH, Gibbs GV (1969) Crystal chemistry of the humite minerals. *Am Mineral* 54:391–411
- Kashin SA (1937) Metamorphism of chromespinellids in the Camel Mountains (southern Urals). In: Fersman AE, Betekhtin AG (eds) *A symposium on the chromite deposits of the USSR*. Acad Sci USSR, Lomonosov Inst (in Russian)
- Mitchell RH (1973) Magnesian ilmenite and its role in kimberlite petrogenesis. *J Geol* 81:301–311
- Mitchell RH (1977) Geochemistry of magnesian ilmenites from kimberlites in South Africa and Lesotho. *Lithos* 10:29–37
- Mitchell RH (1978) Manganian magnesian ilmenite and titanian clinohumite from the Jacupiranga carbonatite, São Paulo, Brazil. *Am Mineral* 63:544–547
- Moore JN, Kerrick DM (1976) Equilibria in siliceous dolomites of the Alta Aureole, Utah. *Am J Sci* 276:502–524
- Müller WF, Wenk HR (1978) Mixed-layer characteristics in real humite structures. *Acta Crystallogr A* 34:607–609
- Murdoch J, Fahey JJ (1949) Geikielite, a new find from California. *Am Mineral* 34:835–838

- Muthuswami TN (1958) Clinohumite, Sausar series, Bhandara District, India. *Proc Indian Acad Sci* 48A:9
- Prins P (1972) Composition of magnetite from carbonatites. *Lithos* 5:227–240
- Rankama K (1938) On the mineralogy of some members of the humite group found in Finland. *Bull Comm Géol Finl* 21:81
- Ribbe PH (1979) Titanium, fluorine, and hydroxyl in the humite minerals. *Am Mineral* 64:1027–1035
- Ribbe PH, Gibbs GV, Jones NW (1968) Cation and anion substitutions in the humite minerals. *Mineral Mag* 36:966–975
- Rice JM (1980) Phase equilibria involving humite minerals in impure dolomitic limestones. Part I. Calculated stability of clinohumite. *Contrib Mineral Petrol* 71:219–235
- Robinson K, Gibbs GV, Ribbe PH (1973) The crystal structures of the humite minerals. IV. Clinohumite and titanoclinohumite. *Am Mineral* 58:43–49
- Sahama TG (1953) Mineralogy of the humite group. *Ann Acad Sci Fenn Ser A3* 31:1
- Trommsdorff V (1966) Beobachtungen zur Paragenese Forsterit (Klinohumit, Chondrodit)-Klinochlor in metamorphen Dolomitgesteinen des Lepontins. *Schweiz Mineral Petrogr Mitt* 46:421–429
- Trommsdorff V, Evans BW (1980) Titanian hydroxyl-clinohumite: formation and breakdown in antigorite rocks (Malenco, Italy). *Contrib Mineral Petrol* 72:229–242
- Wenk E (1963) Klinohumit und Chondrodit in Marmoren der Tessiner Alpen und der Disgrazia-Gruppe. *Schweiz Mineral Petrogr Mitt* 43:287–293
- White TJ, Hyde BG (1982) Electron microscope study of the humite minerals. I. Mg-rich specimens. *Phys Chem Minerals* 8:55–63
- Wise WS (1959) An occurrence of geikielite. *Am Mineral* 44:879–882
- Zhuravleva LN, Berezina LA, Gulín YEN (1976) Geochemistry of rare and radioactive elements in apatite-magnetite ores in alkali-ultrabasic complexes. *Geochem Int* 13:147–166

Accepted May 4, 1987